

The concept of creating thrust based on change angular momentum

Sergei A. Kupreev, Yury N. Razoumny*

Peoples Friendship University of Russia (RUDN University)

Email: kupreev-sa@rudn.ru, razoumny-yun@rudn.ru

Address: 6 Miklukho-Maklaya Street, Moscow, 117198, Russian Federation

Highlights

1. The relationship of rotational and radial movement of the body in the central field
2. Kinetic moment in classical and quantum mechanics
3. Energy efficiency of the motion principle based on the spin
4. The hypothesis about the radiation of particles by the body in the perpendicular plane to the motion
5. An experiment to search for elementary particles with low energy

Keywords: new principle of motion, low energy particles, energy efficiency, motion without overload, quantum gravity test

Abstract: The change in the kinetic moment of a material body is considered regarding to classical and quantum mechanics. The possibility of creating the propulsion system in terms of energy efficiency exceeding the photon engine has been theoretically proved. The proposed new principle of motion is based on the law of conservation of angular momentum and is fully consistent with the basic fundamental laws of physics. It is proposed to use the radiation/absorption of streams of low-energy particles with spin in the direction perpendicular to the movement of the material body. The practical implementation of this idea is confirmed by the presence of promising approaches to solving the problem of quantizing gravity (string theory, loop quantum gravity, etc.) recognized by the world scientific community and by the successful results of experiments conducted by the authors with the motion of bodies in a vacuum chamber. The proposed idea, the examples and experiments has given grounds for the formation of new physical concepts of the speed, mass and inertia of bodies. The obtained results can be used in experiments to search for elementary particles with low energy, to explain a number of physics phenomena and to develop transport of objects based on new physical principles.

1. Introduction

More than a hundred years ago K.E. Tsiolkovsky presented ideas about jet propulsion [1]. For further space exploration, other launch methods are being developed (catapult systems [2], space elevator [3]) and methods of movement in space (orbital skyhook [4], solar sail [5], ion engine [6], laser engine [7], as well as non-reactive EM-Drive engines [8] and Mach effect thruster [9], hypothetical WARP-Drive engine [10], etc.). Even though some of these projects were recognized by world space community as pseudoscientific, the idea of creating new, more efficient propulsion methods is still considered by researchers. The approach to the problem of creating thrust using new physical principles, presented below, are developed in strict compliance with the fundamental laws of physics: the law of conservation of momentum, the law of conservation of angular momentum, the energy conservation law, and the law of conservation of the center of mass position.

The ideas of the controlled motion of a body in the central gravitational field without mass consumption were put forward by specialists in the field of dynamics of orbital tether systems [11-15]. In [11, 12], V.V. Beletskiy proposed the method and model of a spacecraft in the form of a dumbbell, capable of making space flights between coplanar orbits without consuming a working

fluid. A large-sized dumbbell is located in space along the binormal to the orbit so that its center of mass moves along the orbit, in the plane of which the attracting center is located, and the end masses are on opposite sides of this plane. It is shown that by changing the length of the dumbbell bar it is possible to increase the eccentricity of the orbit.

In [13, 14], the dynamical behavior of a tethered connected satellite system during tether length variation is considered. It is shown that appropriate length variation laws can be used to modify the characteristics of the assumed elliptical orbit of the system mass center, as well as to solve the problem of delivering cargo from orbit without consuming fuel.

The monograph [15] proposes control schemes for orbital elements due to different orientations of a dumbbell with a variable bar length, including the use of flywheels to hold the dumbbell in a given position. The idea of using a rotating orbital tether system with a variable bond length is proposed, which is the fact that, due to internal forces, the distance between the end bodies changes and thereby the angular velocity of rotation of the system is controlled so that the system is in the desired orientation longer than in the position, giving the opposite effect of control.

In [16], the orbital elements are controlled by a tether system with a periodically varying length by taking into account the inhomogeneity of the gravitational field.

The internal logic of the development of science prompts to take into account fundamental research in the field of quantum mechanics. The study of the motion essence of material bodies on the basis of the fundamental laws of classical and quantum mechanics opens horizons for a broader understanding of the phenomena of physics and, in particular, for the formation of ideas for creating thrust based on new physical principles.

The purpose of this work is to prove the possibility and energy feasibility of implementing the idea of creating thrust based on a change in the angular momentum. The proof is based on considering the change in the angular momentum of a material body from the point of view of classical and quantum mechanics.

The possibility of creating a propulsion system in terms of energy efficiency exceeding the photon engine is shown. The presented example leads to the hypothesis about the radiation/absorption by the body of elementary particles with spin in the plane perpendicular to the velocity vector of the body. The experiments with the motion of material bodies in a vacuum chamber confirm the hypothesis, put forward and give grounds for the formation of new physical concepts of the speed, mass and inertia of bodies, open up opportunities for the development of transport objects on new principles of motion without mass consumption.

2. Classical mechanics

In the central gravity field, there is a relationship between rotational motion relative to the center of mass of the body and the radial motion of the body [16].

Consider the movement of a rigid dumbbell in the central gravitational field. Suppose that two finite exact masses of a dumbbell m_1 and m_2 are connected by a weightless rigid rod. Two external forces of attraction \mathbf{G}_1 and \mathbf{G}_2 (Fig. 1) are acted upon the dumbbell.

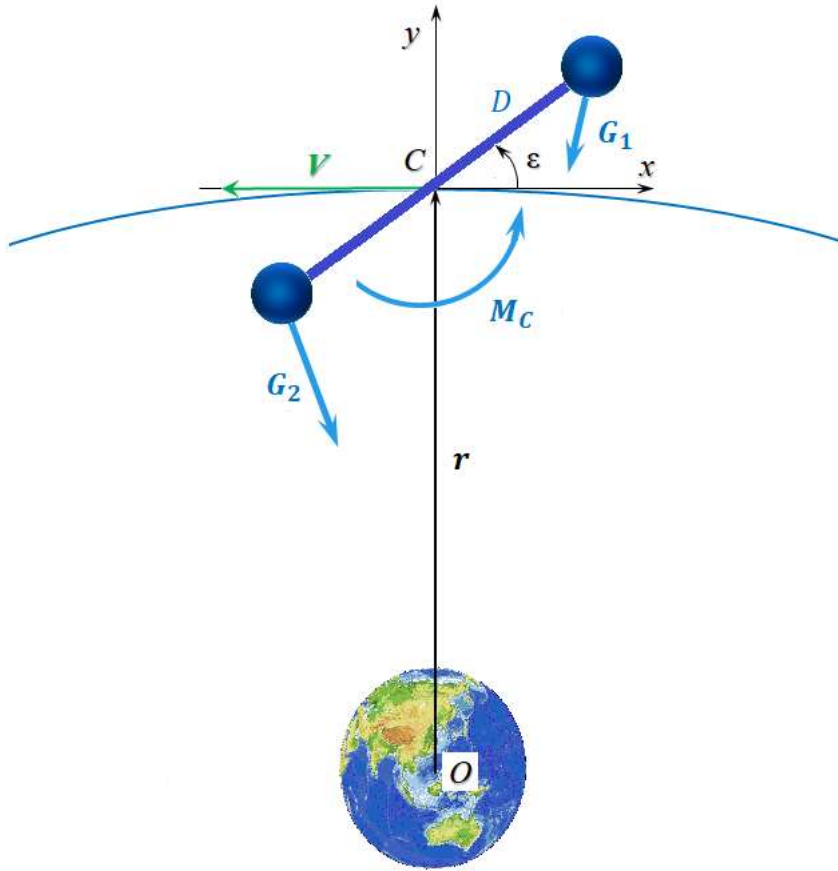


Fig 1. Dumbbell movement in the central gravitational field

The change in the angular momentum of the dumbbell \mathbf{K}_O relative to the center O is equal to the main moment of the external forces \mathbf{M}_O (angular momentum change theorem)

$$\frac{d\mathbf{K}_O}{dt} = \mathbf{M}_O . \quad (1)$$

The moments of attraction forces \mathbf{G}_1 and \mathbf{G}_2 relative to the center O are equal to zero, therefore

$$\mathbf{M}_O = 0, \quad (2)$$

and the angular momentum of the dumbbell \mathbf{K}_O is a constant value.

$$\mathbf{K}_O = \mathbf{K}_e + \mathbf{K}_i; \quad (3)$$

\mathbf{K}_e – the vector of the angular momentum of the mass center of the dumbbell C , in which the entire mass of the dumbbell is concentrated, relative to the center O ;

\mathbf{K}_i – the vector of the angular momentum of the dumbbell rotation relative to the mass center C .

$$\mathbf{K}_e = m \mathbf{r} \times \mathbf{V}; \quad (4)$$

m – dumbbell mass ($m = m_1 + m_2$);;

\mathbf{r} – the radius vector of the mass center of the dumbbell to the attractive center O ;

\mathbf{V} – the velocity vector of the mass center C of the dumbbell.

$$K_i = J_D \Omega; \quad (5)$$

J_D – the moment of inertia of the dumbbell in the plane of motion relative to the center C , the central axial (binormal) moment of inertia;

Ω – absolute angular speed of the dumbbell rotation.

The system of attraction forces \mathbf{G}_1 and \mathbf{G}_2 for a rigid dumbbell is equivalent to the main vector of the system of forces \mathbf{F}_C applied at the center C , and the main moment $\mathbf{M}_C(\mathbf{G}_1, \mathbf{G}_2)$ of forces \mathbf{G}_1 and \mathbf{G}_2 relative to the center C

$$\mathbf{F}_C = \mathbf{G}_1 + \mathbf{G}_2; \quad (6)$$

$$\mathbf{M}_C(\mathbf{G}_1, \mathbf{G}_2) = \mathbf{M}_C(\mathbf{G}_1) + \mathbf{M}_C(\mathbf{G}_2). \quad (7)$$

Let us write equation (6) in projections on the axis of the orbital coordinate system $Cxyz$ (Fig. 2):

$$F_{Cx} = G_{1x} + G_{2x}; \quad (8)$$

$$F_{Cx} = \frac{3}{2} \mu_0 \frac{mD^2}{r^4} \frac{\eta}{(1+\eta)^2} \sin 2\varepsilon; \quad (9)$$

$$F_{Cy} = G_{1y} + G_{2y}; \quad (10)$$

$$F_{Cy} = -\mu_0 \frac{m}{r^2} + 3\mu_0 \frac{mD^2}{r^4} \frac{\eta}{(1+\eta)^2} \sin^2 \varepsilon; \quad (11)$$

ε – the angle between the axis Cx of the orbital coordinate system $Cxyz$ and the line connecting the end elements of the dumbbell;

$\mu_0 = 3,986 \cdot 10^{14} \text{ m}^3/\text{c}^2$ – geocentric gravitational constant of the Earth;

η – the ratio of the end masses of the dumbbell or the distances of the end masses m_1 and m_2 to the center C

$$\eta = m_2 / m_1 = D_1 / D_2. \quad (12)$$

Moment M_C , seeking to return the dumbbell to a position along the local vertical [10]:

$$M_C = \frac{3}{2} \mu_0 \frac{J_D}{r^3} \sin 2\varepsilon; \quad (13)$$

A detailed derivation of expressions (9), (11), and (12) is given in the Appendix.

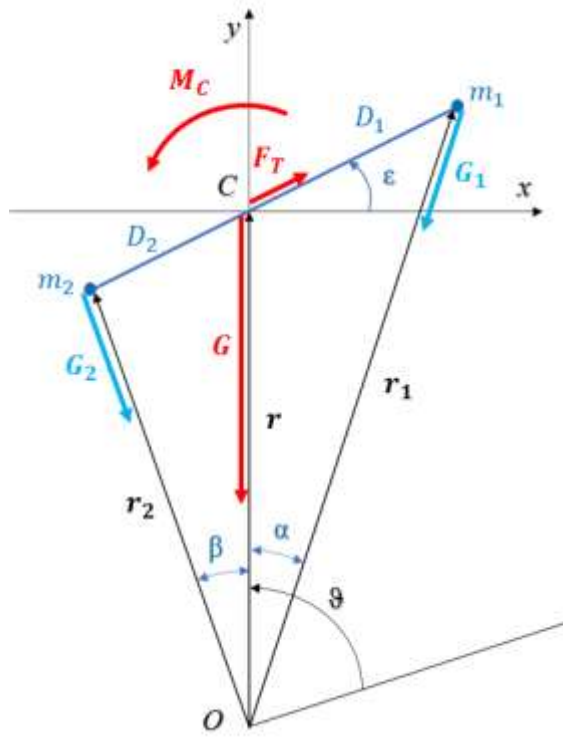


Fig 2. Equivalent systems of forces

Equations (9) and (11) can be represented in the following form:

$$G = \mu_0 \frac{m}{r^2}; \quad (14)$$

$$F_T = 3\mu_0 \frac{mD^2}{r^4} \frac{\eta}{(1+\eta)^2} \sin \varepsilon; \quad (15)$$

G – gravity force at the mass center C , directed along the local vertical towards the center O ;

F_T – thrust at the mass center C , directed along the dumbbell towards the mass m_1 at $\sin \varepsilon > 0$ or towards m_2 at $\sin \varepsilon < 0$ (Fig. 2).

To maintain a given position of the dumbbell at an angle ε , a counterbalancing moment is required, which can be created using a flywheel. The forces of inertia of the flywheel are reduced to a pair of forces with a moment.

$$\mathbf{M}_J = -J\dot{\omega}; \quad (16)$$

J – flywheel moment of inertia;

$\dot{\omega}$ – angular acceleration of the flywheel rotation.

Thus, the system of equations of motion of the mass center C of the dumbbell in the polar coordinate system (r, ϑ) with a flywheel of mass m_j that maintains the angle ε :

$$\ddot{r} - \dot{\vartheta}^2 r = -\frac{\mu_0}{r^2} + 3\mu_0 \frac{D^2}{r^4} \frac{\eta}{(1+\eta)^2} \frac{m}{(m+m_j)} \sin^2 \varepsilon; \quad (17)$$

$$r\ddot{\vartheta} + 2\dot{r}\dot{\vartheta} = -\frac{3}{2}\mu_0 \frac{D^2}{r^4} \frac{\eta}{(1+\eta)^2} \frac{m}{(m+m_j)} \sin 2\varepsilon. \quad (18)$$

On the basis of the system of equations (17) and (18), mathematical modeling of the change in the radius $\Delta r = r_0 - r$ on two orbits was carried out under the initial conditions: $6\,675\text{ km}$, $\dot{\vartheta}_0 = 0.001157689\text{ s}^{-1}$, $D = 100\text{ km}$, $\eta = 1$, $m = m_j$ (Fig. 3). In the case of $\varepsilon = \pi/4$, r decreased by 7 km per one orbit, and in the case of $\varepsilon = 3\pi/4$, it increased by 7 km .

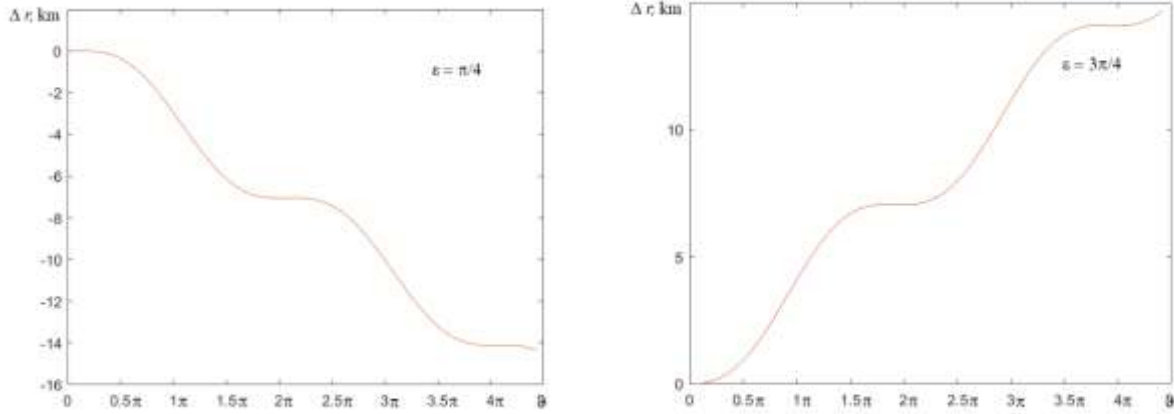


Fig 3. Changing the radial displacement of the dumbbell mass center

As a result, spinning the flywheel to a certain angular velocity ω , the angular momentum \mathbf{K}_i changes, and, consequently, the angular momentum \mathbf{K}_e . The limitation on the maximum change in \mathbf{K}_e is due to the limiting angular velocity of the flywheel rotation.

Fig. 4 shows a diagram of the radial movement of the mass center of the dumbbell C . By changing the direction of the flywheels rotation, the movement of the system can be carried out up (Fig. 4 a) and down (Fig. 4 b). The travel range is limited by the maximum angular speed of the flywheel rotation. Having a group of flywheels with different heights of orbits in one plane, it is possible to implement a scheme for the movement of oncoming traffic flows without fuel consumption. To spin the flywheels, it is enough electricity from power sources (for example, solar panels). However, the technical implementation and efficiency of orbital maneuvers of this scheme [18] is inferior to maneuvers for the exchange of kinetic energy with the use of tether systems technologies [19, 20].

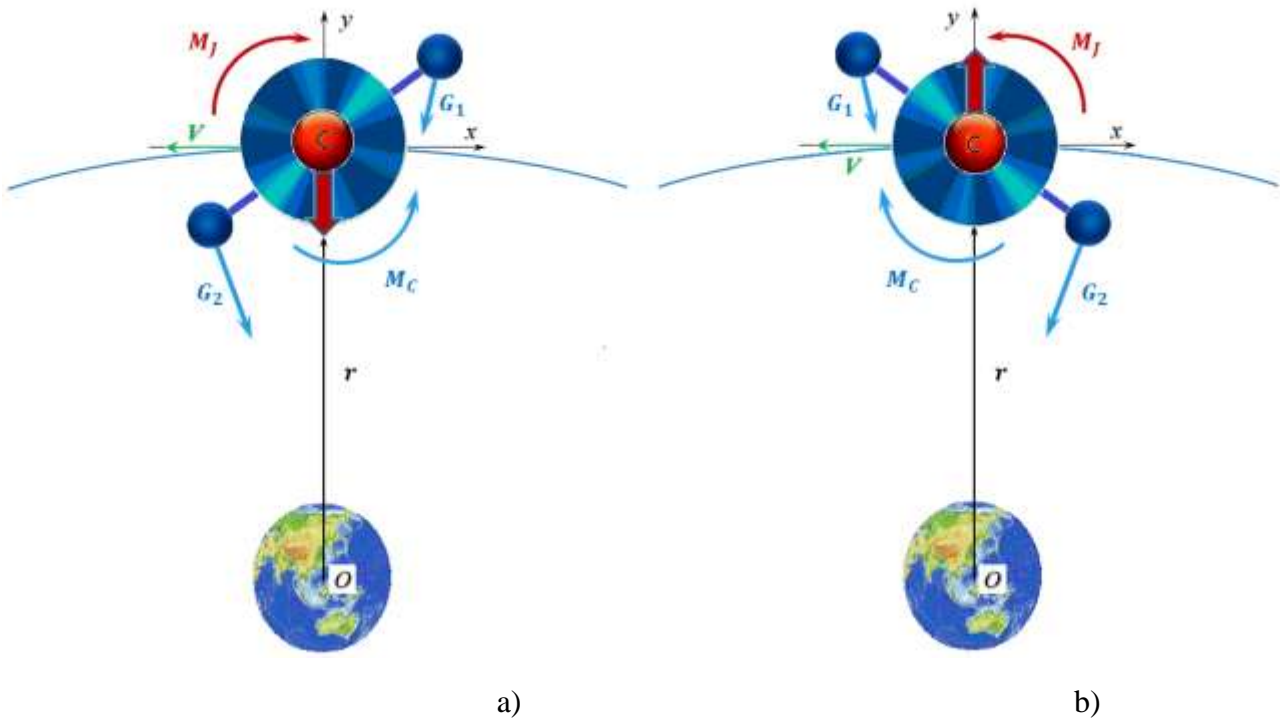


Fig. 4. Scheme of movement in the radial direction

The fact of the relationship between rotational motion around the mass center and radial motion is observed in nature. Every year the Moon moves away from the Earth by 3.8 cm, while the Earth slows down its angular velocity of rotation [21].

Thus, the relationship between the rotational motion of the body relative to the mass center and the radial motion of the body is shown. It should be noted that there is no violation of the conservation law of the mass center position. The center of the gravitational field O (the mass center of a closed system, and more strictly - the mass center of the Earth-dumbbell system), as well as the mass center of the Earth-Moon system, does not change its position. Only the position of the bodies relative to the common mass center changes.

3. Quantum mechanics

It is known from quantum mechanics [22] that elementary particles have spin (intrinsic angular momentum), which has a quantum nature and it is not associated with the movement of the particle as a whole.

Let us use elementary particles as flywheels (Fig. 5). Change in the angular momentum \mathbf{K} of the moved object due to the radiation of n elementary particles

$$\Delta \mathbf{K} = -n \mathbf{s} \frac{h}{2\pi}; \quad (19)$$

\mathbf{s} – the spin vector of an elementary particle;

h – Planck's constant ($h = 6.626070040 \cdot 10^{-34} \text{ J} \cdot \text{s}$).

При этом следует ожидать, что внутренний кинетический момент K_i перемещаемого объекта массой m не изменится (в противном случае получаем раскрытку объекта, которую можно превратить в радиальное движение применяя гантель):

$$\Delta K = \Delta(m \mathbf{r} \times \mathbf{V}) = -n s \frac{h}{2\pi}; \quad (20)$$

In a fairly short period of time

$$\Delta(m \mathbf{r} \times \mathbf{V}) \cong m \mathbf{r} \times \Delta \mathbf{V}_K, \quad (21)$$

$\Delta \mathbf{V}_K$ – the vector of change in the velocity of an object of mass m , in the case of a change in its angular momentum K due to the radiation of n elementary particles.

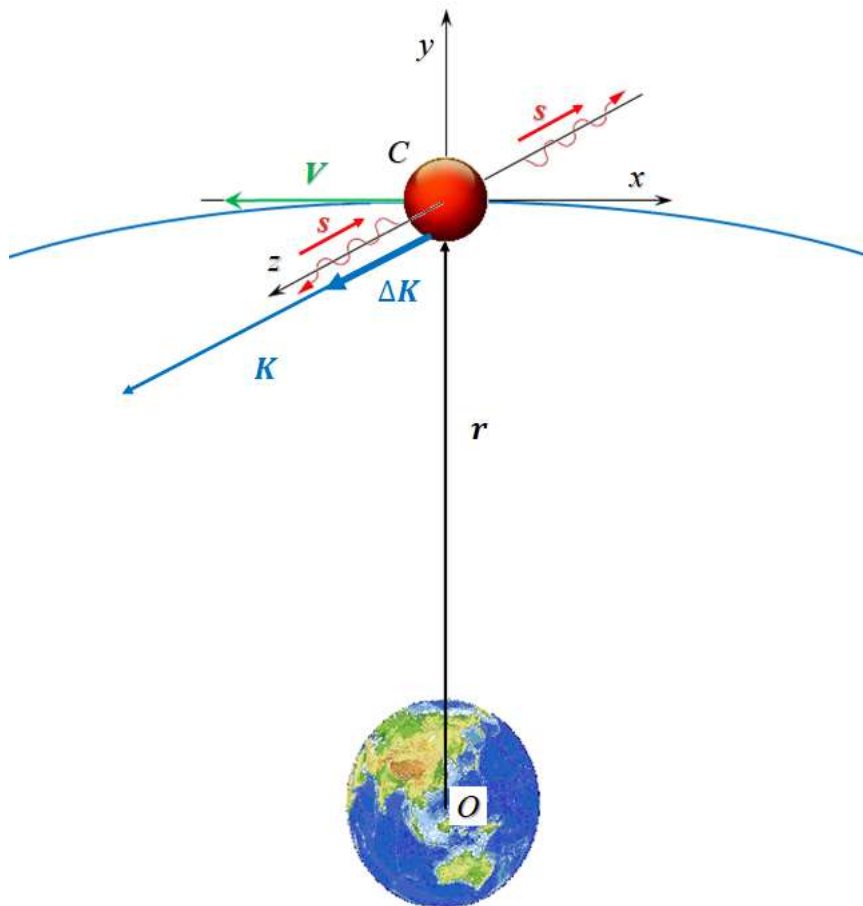


Fig. 5. Motion based on the use of the elementary particles spin

In scalar form

$$m r \Delta V_K \sin(\hat{\mathbf{r}}, \Delta \mathbf{V}_K) = n \frac{s h}{2\pi} \quad (22)$$

In case of $\sin(\hat{\mathbf{r}}, \Delta \mathbf{V}_K) = 1$

$$m \Delta V_K = n \frac{s h}{2\pi r}. \quad (23)$$

Let us consider the last expression from the point of view of energy consumption during movement based on the application of changes in angular momentum and momentum (jet propulsion). To estimate energy costs based on the use of jet propulsion, let us consider a photon

engine that can develop the maximum thrust possible for a jet engine in terms of the expended mass of the moved object.

$$m \Delta V_J = n \frac{h}{\lambda}, \quad (24)$$

ΔV_J – the vector of change in the speed of an object of mass m in the case of jet propulsion due to the radiation of n photons with a wavelength λ . In this case, energy costs for movement:

$$\Delta E_J = n \frac{h c}{\lambda}, \quad (25)$$

where c – the speed of light.

The momentum of the same n photons, using their spin for the movement of an object, is determined by expression (23), and the energy costs for moving an object of mass m :

$$\Delta E_K = n \frac{s h c}{2\pi r}. \quad (26)$$

From expressions (25) and (26) it follows that for $\lambda > 2\pi r/s$, to change the velocity of an object in a central field at a distance R from the center of attraction, it is energetically more advantageous to use the angular momentum of an elementary particle in comparison with its momentum (jet motion). In this case, the radiation of low-energy particles should be carried out in the direction perpendicular to the plane of motion (Fig. 5). The results obtained theoretically prove the possibility and energy feasibility of implementing the idea of creating a thrust based on a change in the kinetic moment for the development of transport facilities based on new physical principles.

Let's evaluate the practical possibility of implementing the idea. In recent decades, several promising approaches to solving the problem of quantizing gravity have been developed: string theory, loop quantum gravity, and others. The proposed theories are confirmed by the observed phenomena in astrophysics and thought experiments. As a consequence of the principle of particle-wave dualism for the description of the gravitational field, the hypothesis of the existence of gravitons is actively considered.

4. Application of gravitons

The Compton graviton wavelength $\lambda_g > 1 \cdot 10^{16}$ m [23], which is much larger than the Earth's radius (6,371,000 m) and the distance from the Earth to the Sun (149,600,000,000 m). Thus, if gravitons are used for motion, then using their spin (angular momentum) is a billion times more profitable than using them in jet motion near the Earth's surface. The spin vector s (direction of radiation) is directed perpendicular to the plane of motion of the object.

Let's estimate the acceleration that the object receives:

$$a = \frac{\Delta V}{\Delta t} = \frac{s h}{2\pi r m \Delta t}. \quad (27)$$

The possibility of controlling quantum processes with an accuracy of up to three attoseconds has been proven ($\Delta t = 3 \cdot 10^{-18}$ s) [24]. Spin graviton $s = 2$. Neutron (proton) mass $1.675 \cdot 10^{-27}$ kg ($m = 1.675 \cdot 10^{-27}$ kg). $r = 6.371 \cdot 10^6$ m. Then acceleration will act on each neutron (proton) $a = 6,600$ m/s².

It is necessary that all atoms of the object simultaneously emit low-energy particles for macroobjects to move with such accelerations without internal deformation. Thus, we get movement without overload. For the practical implementation of the idea, it is necessary to obtain directed flows of low-energy particles.

5. About the law of momentum conservation

An example with gravitons and a diagram of the movement of an object in the radial direction (Fig. 2) give grounds for putting forward the hypothesis about the presence of radiation/absorption of elementary particles with spin.

A material body emits/absorbs elementary particles with spin in a plane perpendicular to the vector of its velocity of motion:

- when the body moves without acceleration, the radiation is equal to the absorption;
- with slow motion of the body, the radiation exceeds the absorption;
- with accelerated motion of the body, the absorption exceeds the radiation.

To estimate the momentum of emitted/absorbed elementary particles, we write equation (23) in the following form:

$$m \Delta V = n \frac{s h}{2\pi \rho}, \quad (28)$$

ρ – the average radius of space curvature in the vicinity of material quantum particles of the body, due to the forces of gravitational attraction of the universe. The use of this scalar parameter in (28) is due to the relationship between the rotational motion of the body relative to the mass center and the radial motion of the body. The specific value of the introduced parameter for the subsequent assessment of the momentum of the emitted/absorbed elementary particles is of no fundamental importance.

An impulse I_r of radiation/absorption

$$I_r = n \frac{s h}{2\pi \rho} \quad (29)$$

appears as a result of a change in the speed of a body and can be transmitted to other bodies. As a consequence, the law of conservation of momentum takes on a broader interpretation: the momentum of the system and the radiation/absorption momentum of elementary particles for a closed system is

a constant value, regardless of the type of interaction of the bodies of the system (elastic or inelastic impact).

As a confirmation of the hypothesis put forward, let us consider a number of examples from different areas of physics and the results of experiments with the motion of bodies in the vacuum.

6. Examples of physic phenomena

Well-known experiment: electron diffraction by a slit (Fig. 6). The appearance of the perpendicular component of the electron momentum after passing through the slit confirms the hypothesis of the presence of radiation/absorption of low-energy particles, and the quantum uncertainty of elementary particles may be due to this radiation.

Radiation of low-energy particles in a plane perpendicular to the electron velocity vector can create the effect of a "pilot wave" and successfully supplement the de Broglie-Bohm theory [25]. The waves created by radiation in a physical vacuum propagate along the direction of motion of the electron: the wave front is in a plane perpendicular to the motion of the electron, and the motion of the wave is directed on opposite sides of the electron. In turn, the physical vacuum affects the process of radiation generation, which leads to known interference patterns, including in the double-slit experiment. The appearance of an observer in the experiment violates the wave structure of the vacuum.

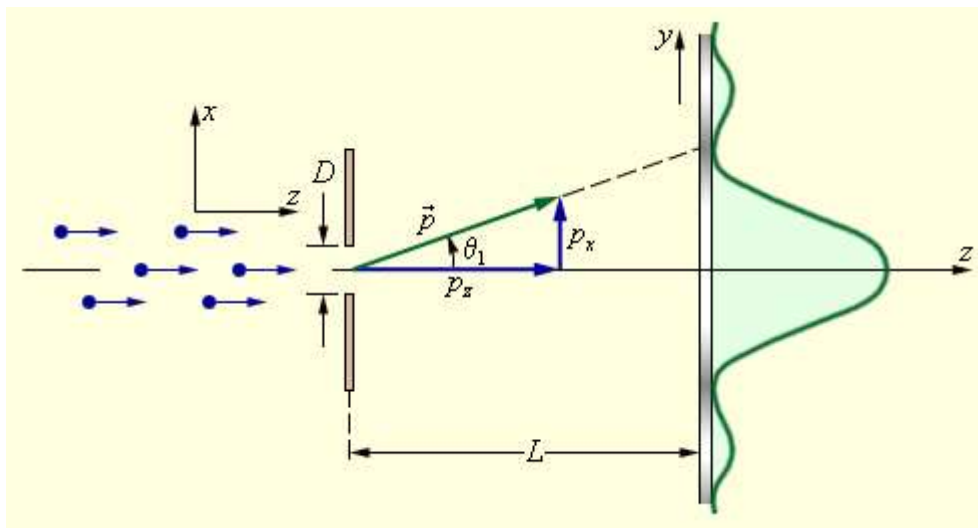


Fig. 6. Diffraction of electrons by the slit

Fig. 7 shows frames from a slow-motion video of a drop falling [26]. As a result of the central inelastic impact, the liquid spreads out in the plane perpendicular to the motion of the drop.

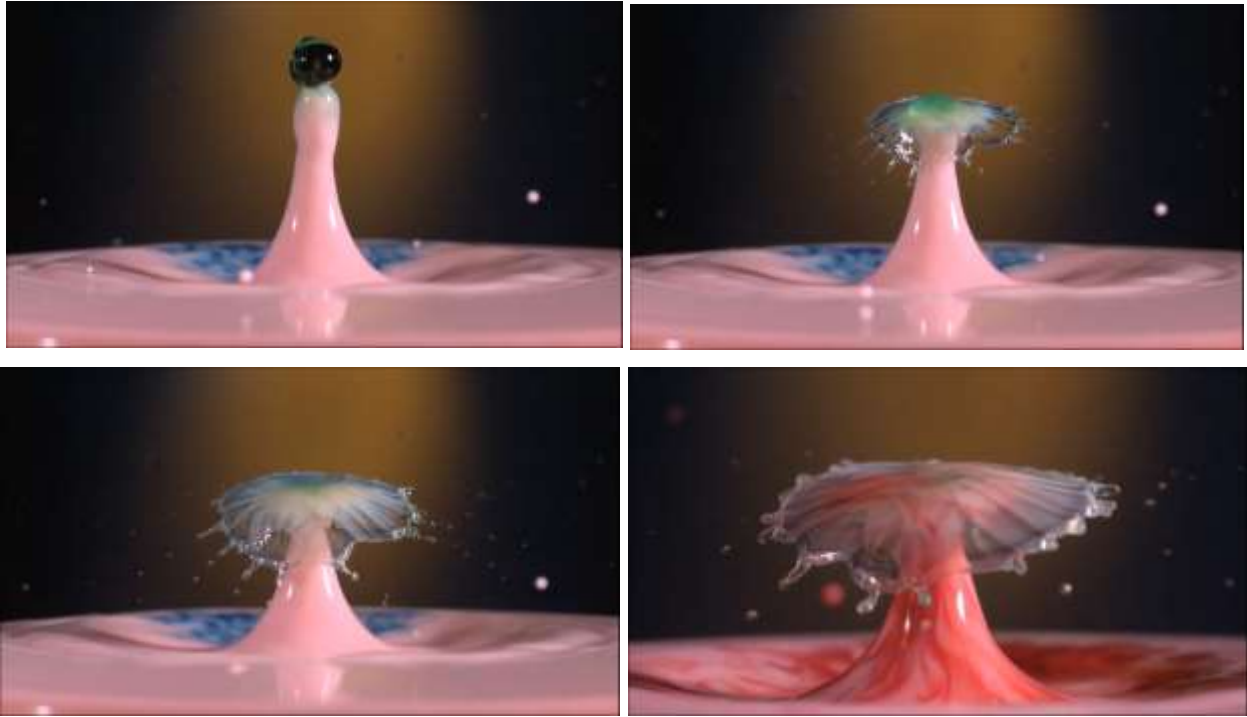


Fig. 7. Central inelastic impact of a liquid drop

In the frames of slow-motion shooting [27] of a pistol shot (Fig. 8), the movement of powder gases in the plane perpendicular to the movement of the bullet is observed.



Fig. 8. The direction of movement of gases after the shot

The given examples clearly demonstrate the transition of the momentum of bodies into a plane perpendicular to the initial motion of the body. These examples are quite consistent with the hypothesis put forward.

To confirm the hypothesis about the presence of radiation/absorption of elementary particles in the process of accelerated motion of the body, it is advisable to carry out experiments in a vacuum.

7. American experiment

On the Internet there is a popular experiment with gravity, which was conducted by physicist Brian Cox in a large vacuum chamber "Space Power Facility" NASA in the US state of Ohio [28].

Fig. 9 shows the time-lapse footage of the fall of a lead ball and a feather in a vacuum. Let us pay attention to the movement of villi against the center of the ball.

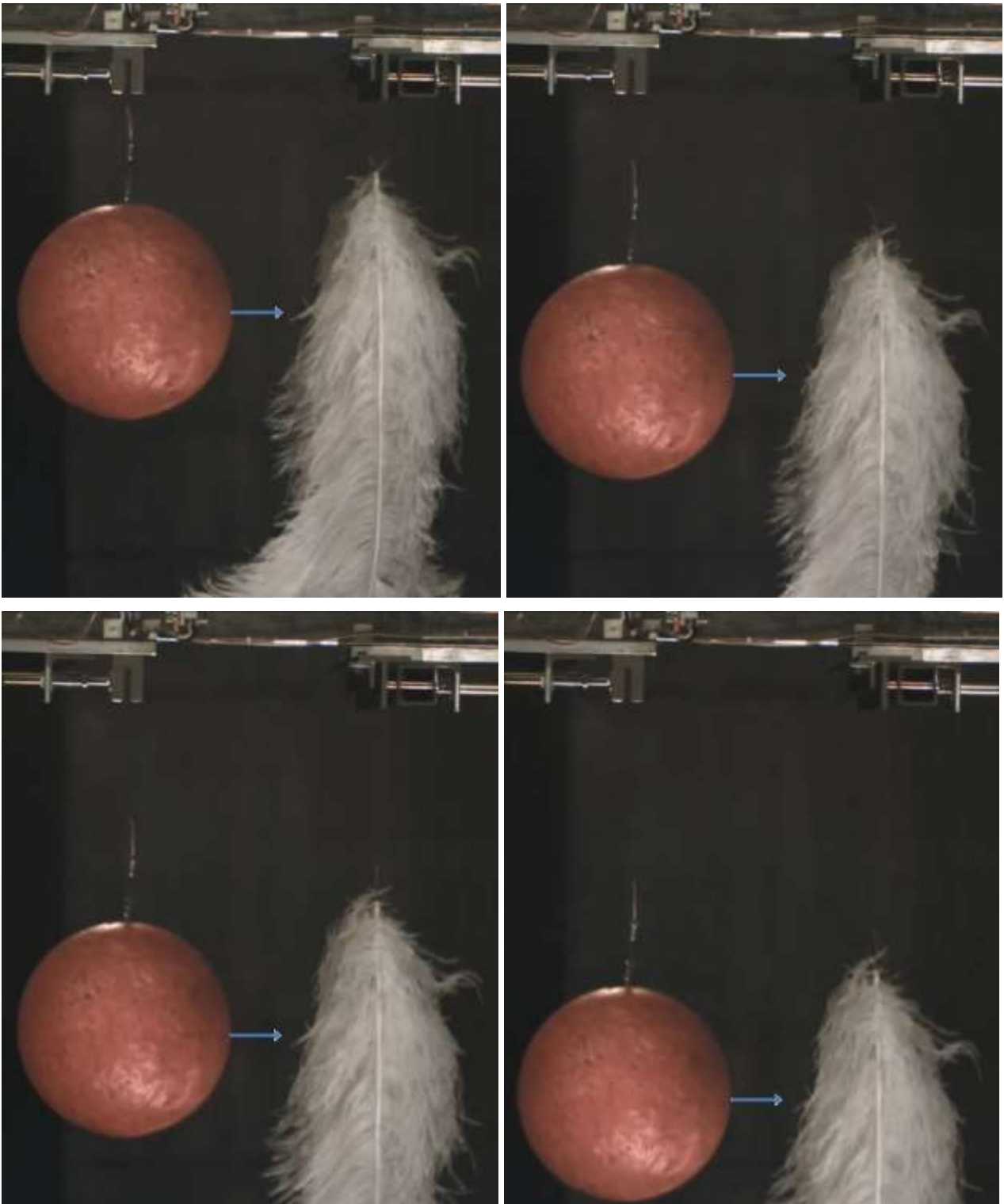


Fig. 9. Footage of a lead ball and feather falling in vacuum

After the simultaneous release of the ball and feather from the attachment in the first moments of falling on the video recording of the experiment [28], the movement of the feather villi is observed, due to their elastic properties during the transition from the suspended state of the feather to

weightlessness (free fall). In subsequent moments, the movement of the feather villi facing the center of the ball differs from the general movement of the remaining villi. The nature of the movement of the villi, which the arrow points to (Fig. 9), confirms the assumption about the presence of absorption by the ball of elementary particles in the plane perpendicular to its movement (Fig. 10). In fig. 10 arrows in the plane indicate the direction of motion of elementary particles towards the mass center of the ball.

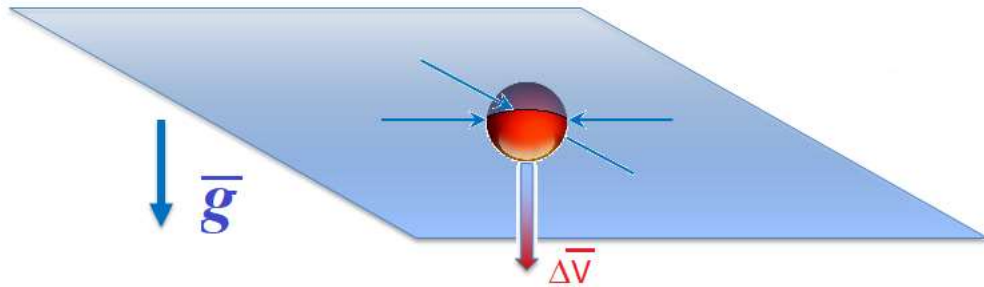


Fig. 10. Directions of motion of elementary particles in the case of accelerated motion

The process of ball rebound from the damper is also under the study. In this case, when the ball moves up, the presented frames of slow motion (Fig. 11) coincides with the assumption that the ball emits elementary particles in the plane perpendicular to its motion.



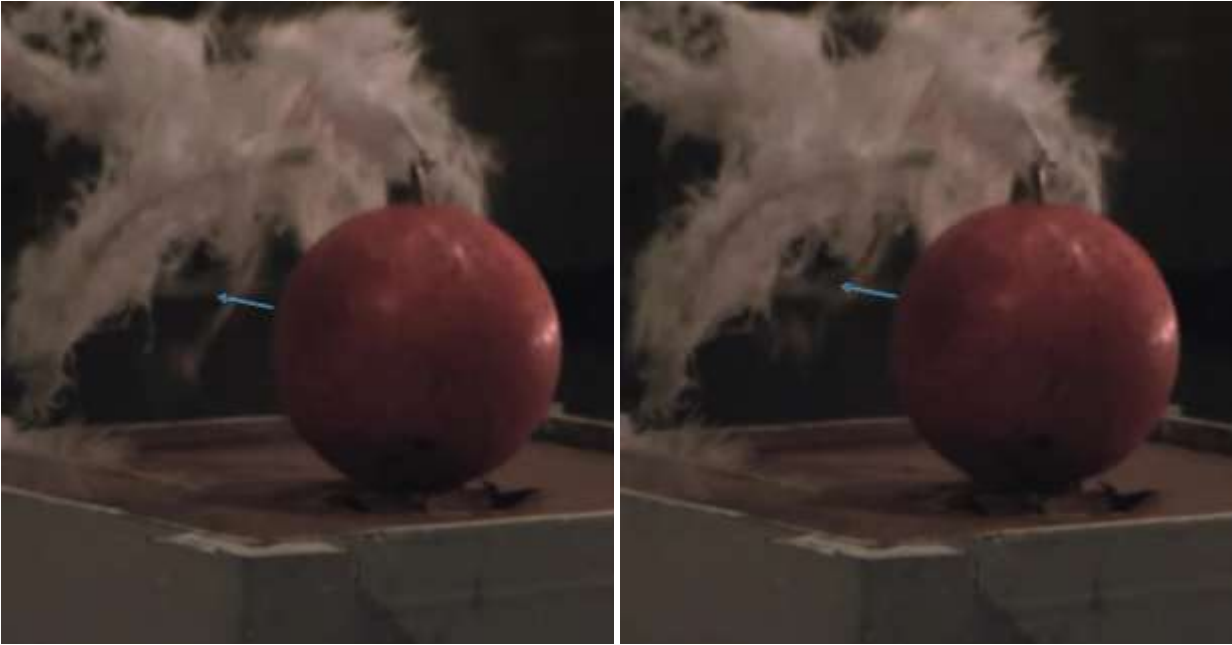


Fig. 11. Frames of the rebound of the ball and feathers in vacuum

The directions of motion of elementary particles from the mass center of the sphere are indicated by arrows in the plane in Fig. 12.

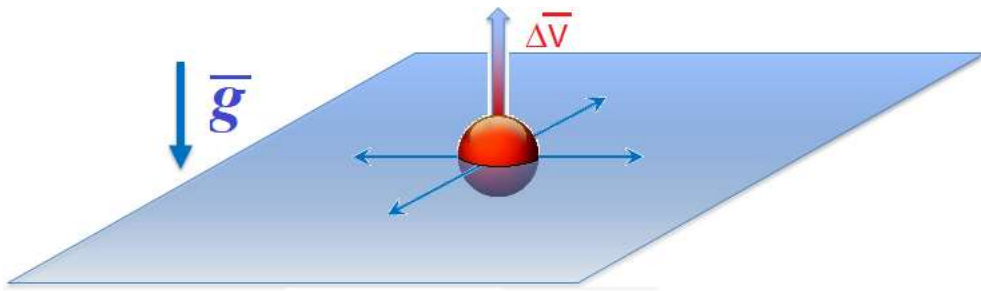


Fig. 12. Directions of movement of elementary particles in the case of slow motion

In the above experiment, feathers play the role of a detector that records the flow of passing elementary particles. The number of these n_d particles can be estimated based on the equation (28):

$$n_d = m \Delta V \frac{2\pi \rho}{s h} \cdot \frac{d V \Delta t}{2\pi l V \Delta t} = m \Delta V \frac{\rho d}{s h l} ; \quad (30)$$

V – the speed of the body (ball) relative to the detector (Fig. 13);

Δt – the time interval during which the speed of the body (ball) changes by ΔV with respect to the detector;

d – width of the detector (villi) in the plane of radiation/absorption by the body (ball) of elementary particles (Fig. 13);

l – the distance from the detector (villi) to the mass center of the ball (Fig. 13).

Thus, the area $A = d \cdot V \cdot \Delta t$ crosses n_d elementary particles in time Δt .

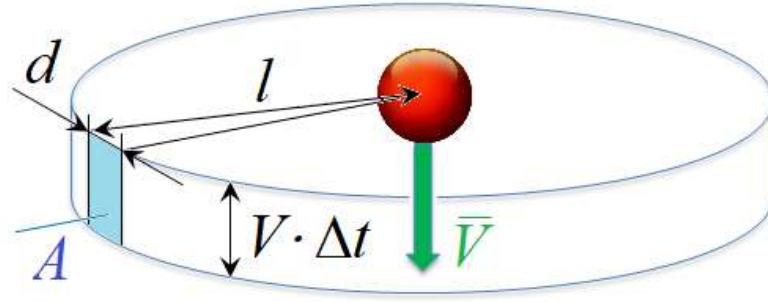


Fig. 13. Scheme for calculating the particle flux through detector A

In the case of a free fall of a body (ball) with acceleration g , the dependence of the change in velocity ΔV on the change in the height of the ball ΔH is determined as follows:

$$\Delta H = V_0 \cdot \Delta t + \frac{g \cdot \Delta t^2}{2}, \quad \Delta V = g \cdot \Delta t, \quad (31)$$

where V_0 – the initial speed of the body – (ball);

$$\Delta H = \frac{V_0 \cdot \Delta V}{g} + \frac{\Delta V^2}{2 \cdot g}; \quad (32)$$

$$\Delta V = \sqrt{V_0^2 + 2g \Delta H} - V_0. \quad (33)$$

Then, taking into account (30) and (33), the number of particles n_d passing through the detector with height ΔH is

$$n_d = m \frac{\rho d}{s h l} \left(\sqrt{V_0^2 + 2g \Delta H} - V_0 \right). \quad (34)$$

The function $n_d(V_0)$, defined by expression (34), for positive values of ΔH has a negative derivative: $n'_d(V_0) < 0$, therefore, the function $n_d(V_0)$ is decreasing, and its maximum value is attained at $V_0 = 0$:

$$n_{d \max} = m \frac{\rho d}{s h l} \sqrt{2g \Delta H}. \quad (35)$$

Let us estimate the Compton wavelength of an elementary particle based on the principle of equivalence of mass and energy.

When the speed of a body changes, its relativistic mass changes:

$$\Delta m = m_{rel} - m = m \left(\frac{1}{\sqrt{1 - \frac{\Delta V^2}{c^2}}} - 1 \right) = m \frac{\Delta V^2}{2 c^2}, \quad (36)$$

Based on the energy conservation law, the radiation energy of elementary particles E with the Compton wavelength λ

$$E = n h \nu = n h \frac{c}{\lambda} \quad (37)$$

cannot exceed the change in the energy of the body due to the relativistic effect:

$$n h \frac{c}{\lambda} \leq \Delta m c^2 . \quad (38)$$

Taking into account equations (28) and (36), we obtain

$$\frac{c}{\lambda} \leq \frac{s \Delta V}{4 \pi \rho} . \quad (39)$$

The maximum value $\Delta V = c$ and inequality (39) takes the form

$$\lambda \geq \frac{4 \pi \rho}{s} . \quad (40)$$

Constraint (40) can only be satisfied by very low-energy particles. For example, the Compton wavelength of a hypothetical particle graviton $\lambda_g > 1 \cdot 10^{16}$ m [23].

8. The Russian experiment

Low-energy particles, satisfying condition (40), have energy far beyond the measurement error of the Large Hadron Collider. However, according to the given hypothesis, there is radiation from a stream of low-energy particles with spin. The difference in the number of particles n_d between the number of emitted and absorbed body particles is determined by expressions (30), (34) or (35). In these expressions, there is a change in the body's velocity ΔV with respect to the detector or a change in height ΔH and an acceleration g , i.e. a relative accelerated motion is required between the detector and the body to register the radiation.

To detect the flow of these particles, the authors carried out an experiment on the basis of the "Scientific Testing Center of the Rocket and Space Industry" (STC RSI) of the State Corporation "Roscosmos" in the vacuum chamber with a volume of 4 m^3 (diameter 1.6 m, length 2 m). In the upper part of the vacuum chamber, a mechanical, electrically driven device for the simultaneous release of a cast-iron ball weighing 7.26 kg with a diameter of 11 cm, a bundle of ostrich feathers and a GoPro 8 HERO Black video camera providing slow-motion shooting with a frequency of 240 frames per second in HD. A garland of ostrich and decorative feathers on a cotton thread (radiation detector) was placed on an independent suspension in the form of a steel wire (removes a static charge) next to the ball's fall path. The vacuum chamber also contained a stationary video camera, a tripod with vertically positioned halogen car lamps, rubber mats to dampen the impact of the ball, and green polyurethane mats to ensure the quality of shooting (Fig. 14)



Fig. 14. Equipment for the experiment in the vacuum chamber of the STC RSI

A video recording of the ball falling from a height of 1.1 m made by stationary and mobile GoPro video cameras in vacuum conditions. The ball was dropped four times.

During the first attempt, a small decorative feather with a steel ring was dropped for attachment to the release device. The feather served as an indicator of the purity of the vacuum – the feather fell in front of the ring. The pressure in the chamber was 0.08 mm Hg. The drop device worked normally, but the mobile video camera failed. The backlight consisted of two car lamps, which influenced the low brightness of the shooting. Additionally, panoramic shooting was carried out on the iPhone 8 from the outside through the porthole of the vacuum chamber. Using a stationary GoPro camera, it was possible to record the attraction of the feather by the ball at the final stage of the fall at the bottom of the garland (Fig. 15). When the ball moves, a change in the angle of the feather of a stationary garland opposite the center of the ball is recorded. This fact is consistent with the diagram in Fig. 10. The purity of the experiment is questioned by the touch of a falling feather in the middle of the garland.





Fig. 15. Fragments of video recording frames. Changing the angle of the fluff relative to the vertical: a) before the flight of the ball, b) during the flight of the ball

During the second attempt, the drop device and video cameras worked normally. The backlight consisted of four automotive lamps arranged vertically along a stand. The pressure in the chamber was 0.08 mm Hg. A bunch of ostrich feathers were dropped. At the moment of transition from a suspended state to a state of weightlessness (falling), the fluffs move relative to the ball (there is ΔV). The advantage of this type of motion is that there is no gravity load on the fluff and that the maximum flow of low-energy particles is ensured (21). A clear anomaly in the movement of feathers against the center of the ball is observed in the American experiment described above (Fig. 9). In the presence of attraction from the side of the ball, the oscillation period of the fluffs close to the horizontal plane of the section passing through the mass center of the ball should decrease. The presented frames from the GoPro mobile camera show the oscillation of a fluff close to the above plane (Fig. 16). The frequency of its oscillations is higher than that of the others: the fluff manages to make two complete oscillations, while the rest is no more than 1.5. In the first frame (Fig. 16 a), the fluff is deflected by the maximum amplitude from the vertical. In the second frame (Fig. 16 b), the fluff is pressed back to the feather.



a)



b)



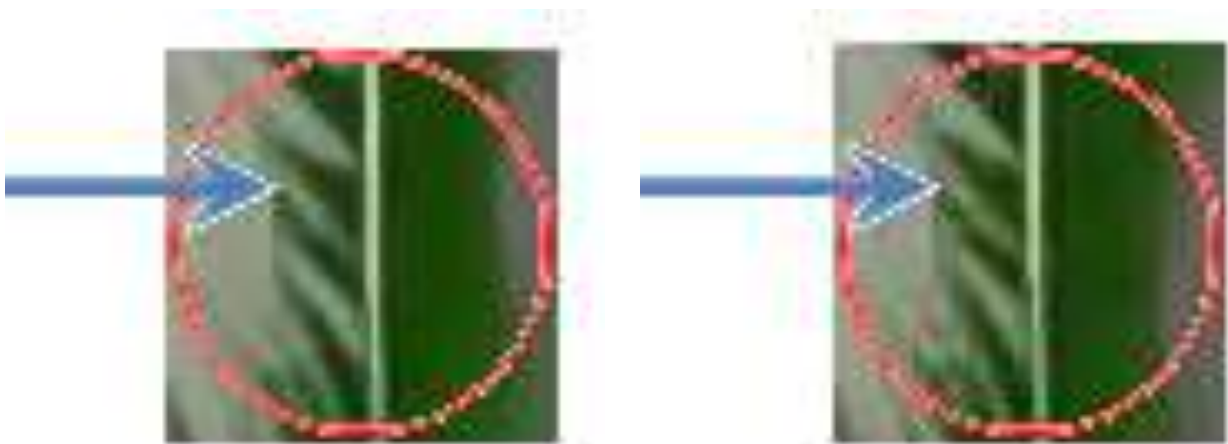
c)



d)

Fig. 16. Video footage of a fall of the ostrich feathers bunch from a falling video camera

In the third frame (Fig. 16c), the fluff again deflects to its maximum amplitude (somewhat less than in the first frame - damped oscillations) towards the ball. In the fourth frame (Fig. 16d), the fluff again tends to the vertical. In the same frame, a new fluff appears for the first time, clearly opposite the center of mass of the ball, slightly lower than the previously considered fluff. Its appearance may be due to the presence of radiation of low-energy particles in the direction of the ball, in particular, this radiation could serve as a trigger when removing it from the engaged position.



a)

б)

Fig. 17. Frames and fragments of video recordings of the change in the position of the fluff relative to the vertical: a) before the flight of the ball, b) after the flight of the ball

Video footage of the ball falling and the deflection of the garland fluffs from a stationary (suspended on an independent thread) GoPro video camera was obtained (Fig. 17 – 19).

When comparing fragments of frames (Fig. 17) before and after the flight of the ball next to the fluff (indicated by the arrow), its deviation towards the ball is observed. Similar deflections of fluffs are observed at other moments of the ball's falling (Fig. 18 and Fig. 19).

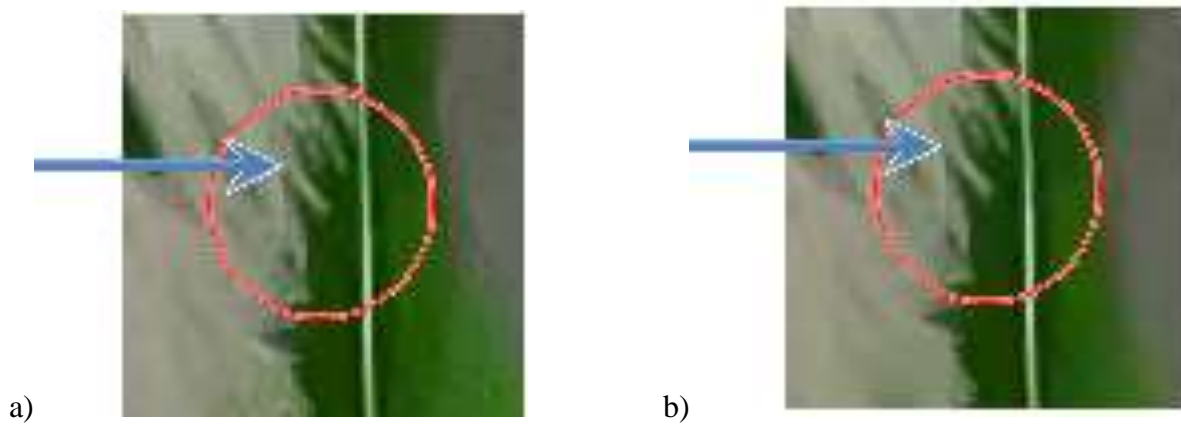


Fig. 18. Frames and fragments of video recordings of the change in the position of the fluff relative to the vertical: a) before the flight of the ball, b) after the flight of the ball

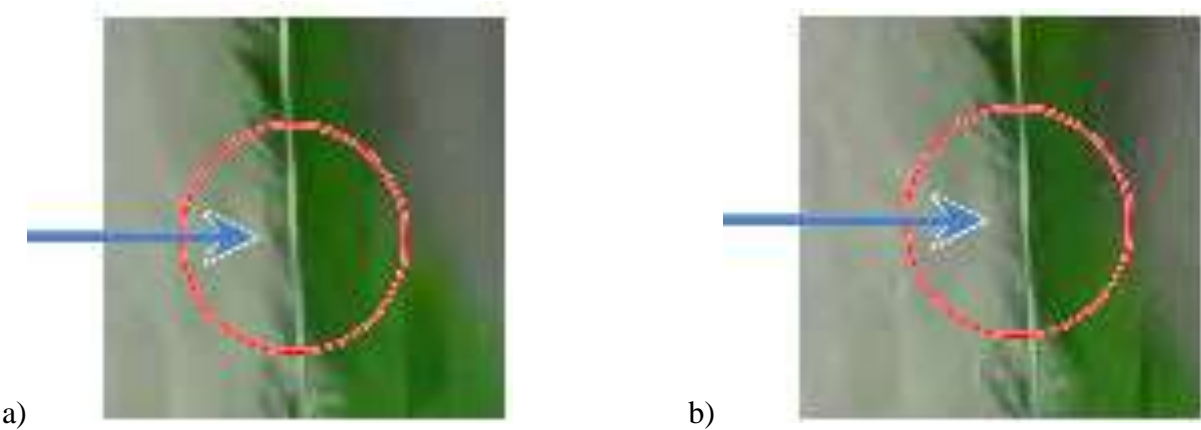
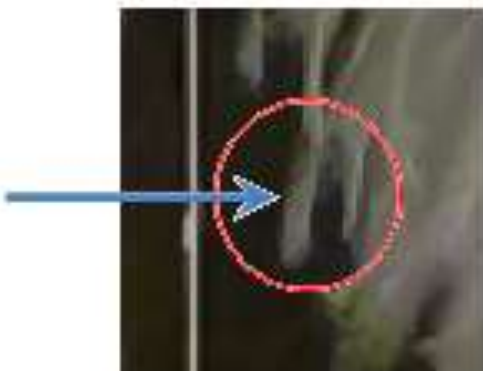
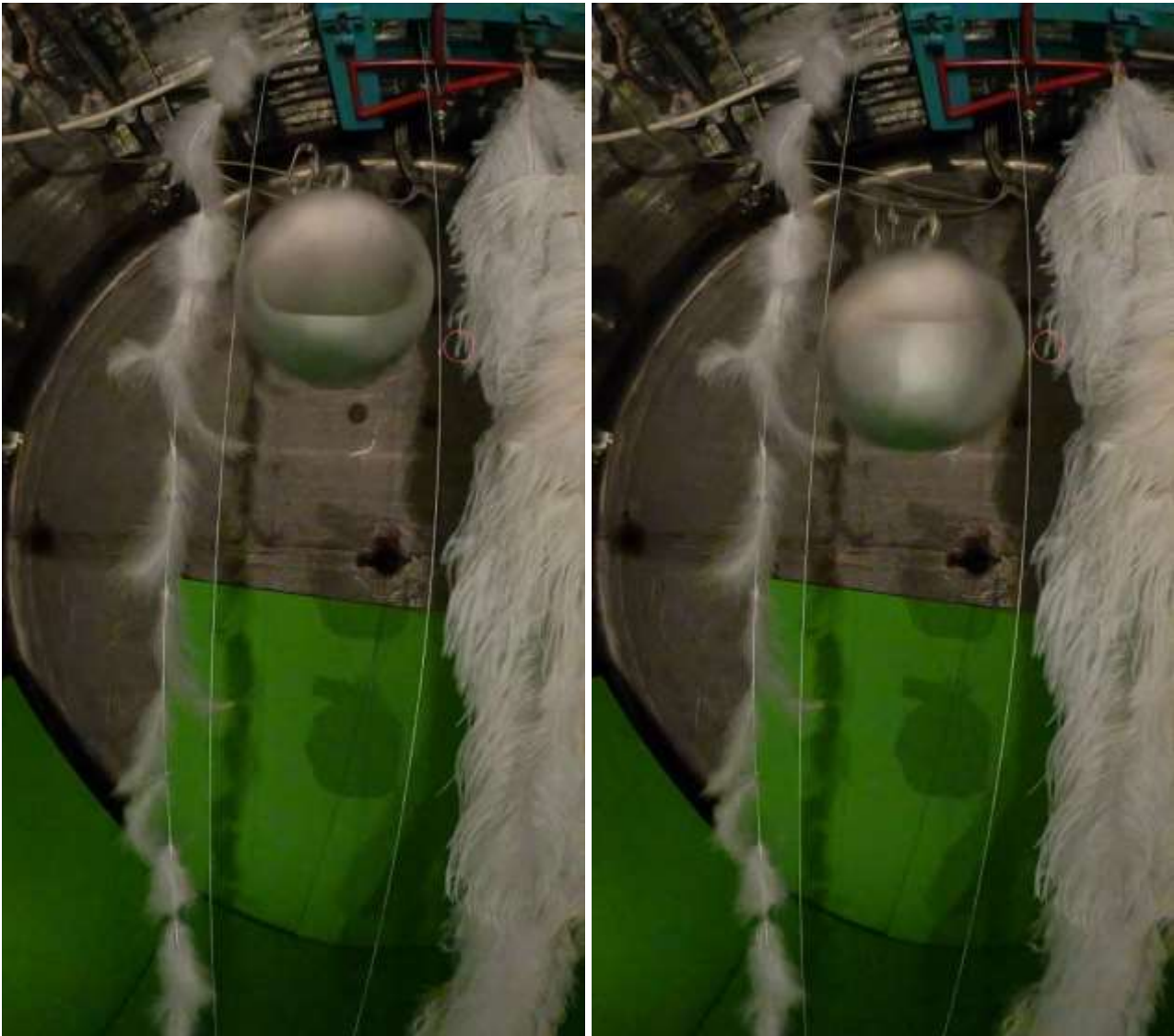


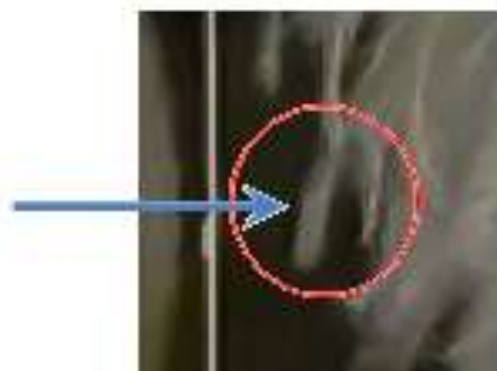
Fig. 19. Frames and fragments of video recordings of changes in the position of fluffs:
a) before the flight of the ball, b) after the flight of the ball

On the third attempt, the chamber pressure was 0.07 mm Hg. Both cameras were stationary (they were hung on threads). Two vertical plumb lines, a garland of decorative feathers (left) and a garland of ostrich feathers (right) were located along the flight path of the ball on different sides (Fig. 20). When falling, the ball touched the decorative feathers of the left garland; therefore, the analysis

of the movement of the feathers of the decorative feathers is not given. The right garland was lightly hit by the ejector lever. The maximum amplitude of feathers in the upper and middle parts of it (closest to the trajectory of the ball's fall) was observed at the moment when the ball mass center passed (Fig. 20). It is easier for the radiation flux to amplify the oscillations of the detector than to bring it out of its rest state. In other words, it is easier for the radiation flux to bypass a stationary obstacle. The radiation flux does not have time to respond to changes in the vacuum in the event of detector oscillations.



a)



b)

Fig. 20. Frames and fragments of changing the fluff position relative to the vertical: a) before the flight of the ball, b) after the flight of the ball

On the fourth attempt, the chamber pressure was 0.16 mm Hg. Two vertical plumb lines, a garland of large ostrich feathers and two garlands (one of decorative, the other of ostrich) feathers were located along the flight path of the ball on opposite sides. Each garland was weighted with a weight (20 mm iron nut) at the lowest point. Subtle deviations of the fluffs of the garlands were observed opposite the center of the falling ball.

The ball bounced about 30 cm after a strong impact on the damper at the bottom of the vacuum chamber. This circumstance influenced the conditions of the experiment and did not allow testing the hypothesis in terms of body radiation.

The authors plan to conduct an experiment in a vacuum chamber 8 m high on the basis of STC RSI using higher-speed video cameras. From equations (34) and (35) it follows that the maximum effect from the radiation of low-energy particles should be observed at $V_0 = 0$ and large accelerations. Therefore, special attention will be paid to the beginning of the fall ($V_0 = 0$), the moment of the rebound when hitting the damper (large acceleration) and the moment the ball hovers in the upper part of the trajectory after the rebound (change in the direction of radiation of low-energy particles). It is supposed to study the movement of bodies of various shapes, including disc-shaped and cigar-shaped.

The numerous examples of the movement of fluffs in a vacuum given in this section, obtained as a result of each of the four drops of the ball in the framework of the experiment on the basis of the STC RSI, are consistent with the given hypothesis. The authors invite interested researchers to conduct a similar experiment.

9. Massless engine technology

According to the proposed hypothesis, a device creating thrust without mass consumption should provide high-frequency oscillations of the working fluid and receive a useful flow of low-energy elementary particles with spin. The most famous attempts to implement such devices are EM-Drive Thruster [29, 30] and Mach effect thruster [31].

It is necessary to carry out additional experiments in order to study the generation of directed flows of low-energy elementary particles and the possibility of their reception to create more efficient devices. Different directions and intensities of low-energy particle fluxes are expected for working bodies of different shapes. Receiving useful low-energy fluxes, forming thrust, is achieved by moving the receiver in the direction of radiation of particles at the time of their generation and subsequent removal of the receiver when changing the direction of radiation.

10. About the law of angular momentum conservation

Taking into account the hypothesis, the movement of a dumbbell with a flywheel (Fig. 3) can be considered as follows:

$$\mathbf{K}_{i1} = \mathbf{K}_{i0} + \mathbf{K}_r, \quad (41)$$

which does not contradict the law of angular momentum conservation of the system \mathbf{K}

$$\mathbf{K} = \mathbf{K}_{i0} + \mathbf{K}_{e0} = \mathbf{K}_{i1} + \mathbf{K}_{e1} = (\mathbf{K}_{i0} + \mathbf{K}_r) + \mathbf{K}_{e1} = \mathbf{K}_{i1} + (\mathbf{K}_{e0} - \mathbf{K}_r), \quad (42)$$

where \mathbf{K}_{i0} , \mathbf{K}_{i1} – the initial (at time t_0) and final (at time t_1) vectors of the internal angular momentum relative to the mass center of the dumbbell C ,

\mathbf{K}_{e0} , \mathbf{K}_{e1} – the initial (at time t_0) and final (at time t_1) angular momentum vectors of the mass center of the dumbbell C ,

\mathbf{K}_r – the vector of the angular momentum of radiation (or absorption) of elementary particles over time $\Delta t = t_1 - t_0$ due to the accelerated rotation of the flywheel.

This representation of the angular momentum of a body allows a more in-depth explanation of the phenomenon of radial displacement of the mass center C in the central gravitational field.

It is advisable to conduct an experiment in space according to the scheme (Fig. 3) to detect directional radiation along the axis of flywheel rotation (“jet”) and understand the mechanism of formation of jets from an accretion disk in astrophysics.

11. About the theory of quantum gravity

The demand for consistency between a quantum description of matter and a geometric description of spacetime a theory is required in which gravity and the associated geometry of spacetime are described in the language of quantum physics. Despite major efforts, no complete and consistent theory of quantum gravity is currently known, even though a number of promising candidates exist.

Among the majority of modern theories of gravity, the theory of gravity with torsion is recognized as an extension of the general theory of relativity [32]. Currently, there are active attempts to construct a quantum theory of gravity, the main directions are considered to be string theory [33] and loop quantum gravity [34]. The main problem in confirming the proposed theories is the difficulty in conducting experiments to search for low-energy particles [35, 36].

The last well-known experiments with gravity were carried out in two main directions [37]:
 1) measurement of the force of gravitational attraction between material bodies [38, 39, 40, 41, 42];
 2) measurements of gravitational waves (changes in the gravitational field, space-time) [43, 44]; and are not associated with the registration of low-energy particle fluxes interacting with material bodies. A similar interaction is observed in astrophysics (the phenomenon of "dark matter") [45]. In case of proper experimental confirmation, the given hypothesis about the radiation/absorption of low-energy particles by bodies will make it possible to establish a connection between gravity and the physics of the microworld, classical and quantum mechanics.

The given hypothesis is consistent with the basic laws of physics: the law of conservation of momentum, the law of conservation of angular momentum, the law of conservation of energy, and the law of conservation of the position of the mass center.

As regards the latter, it should be noted that it does not hold in relativistic mechanics. Let's look at a simple example. Two bodies of different masses, forming a closed system, move in a straight line towards each other, for example, by gravity. The speed of an object with a smaller mass increases more than that of another object, i.e. its relativistic mass increases faster (36). This means that the mass center of the system shifted towards the object with a smaller mass. In the case of the given hypothesis, the mass center of the system does not change due to the inclusion of radiation.

12. Conclusion

- 1) The possibility and energy feasibility of implementing the idea of creating a thrust based on a change in the kinetic moment for the development of transport objects based on the new physic principles has been theoretically proved.
- 2) The practical implementation of the idea requires additional fundamental research and experimental confirmation of the fluxes of low-energy elementary particles with spin.
- 3) The proposed hypothesis, the given examples and experiments give grounds for the formation of new physic concepts of the speed, mass and inertia of bodies.
- 4) The results obtained can be used in experiments to search for low-energy elementary particles.
- 5) Devices creating thrust without mass consumption should provide high-frequency oscillations of the working fluid and receive a useful flow of low-energy elementary particles with spin.

Acknowledgments

This paper has been supported by the RUDN University Strategic Academic Leadership Program.

Author Declarations

The authors have no conflicts to disclose.

Data availability

The data that support the findings of this study are available from the corresponding author upon reasonable request.

Appendix. Calculation of forces and moments in the orbital coordinate system

Modules of gravity forces G_1 and G_2

$$G_1 = \mu_0 \frac{m_1}{r_1^2}; \quad G_2 = \mu_0 \frac{m_2}{r_2^2}. \quad (43)$$

Projections of gravity forces G_1 and G_2 on the Cx axis (Fig. 2):

$$G_{1x} = -G_1 \sin \alpha ; \quad G_{2x} = G_2 \sin \beta . \quad (44)$$

By the sine theorem

$$\frac{\sin \alpha}{D_1} = \frac{\sin(\pi/2 + \varepsilon)}{r_1}; \quad \frac{\sin \beta}{D_2} = \frac{\sin(\pi/2 - \varepsilon)}{r_1}; \quad (45)$$

$$\sin \alpha = \frac{D_1}{r_1} \cos \varepsilon; \quad \sin \beta = \frac{D_2}{r_2} \cos \varepsilon; \quad (46)$$

Projections of gravity forces \mathbf{G}_1 and \mathbf{G}_2 on the Cy axis (Fig. 2):

$$G_{1y} = -G_1 \cos \alpha; \quad G_{2y} = -G_2 \cos \beta; \quad (47)$$

where

$$\cos \alpha = \frac{r + D_1 \sin \varepsilon}{r_1}; \quad \cos \beta = \frac{r - D_2 \sin \varepsilon}{r_2}. \quad (48)$$

From (44), (45) and (46) and taking into account $m_1 D_1 = m_2 D_2$ (12) we successively obtain

$$F_{Cx} = -G_1 \sin \alpha + G_2 \sin \beta; \quad (49)$$

$$F_{Cx} = -\mu_0 \frac{m_1 D_1}{r_1^2} \cos \varepsilon + \mu_0 \frac{m_2 D_2}{r_2^2} \cos \varepsilon; \quad (50)$$

$$F_{Cx} = \mu_0 m_1 D_1 \cos \varepsilon \left(\frac{1}{r_2^3} - \frac{1}{r_1^3} \right). \quad (51)$$

From (47) and (48)

$$F_{Cy} = -G_1 \cos \alpha - G_2 \cos \beta; \quad (52)$$

$$F_{Cy} = -\mu_0 \frac{m_1 (r + D_1 \sin \varepsilon)}{r_1^2} - \mu_0 \frac{m_2 (r - D_2 \sin \varepsilon)}{r_2^2}; \quad (53)$$

$$F_{Cy} = -\mu_0 \frac{m_1 r}{r_1^3} - \mu_0 \frac{m_1 D_1 \sin \varepsilon}{r_1^3} - \mu_0 \frac{m_2 r}{r_2^3} + \mu_0 \frac{m_2 D_2 \sin \varepsilon}{r_2^3}; \quad (54)$$

$$F_{Cy} = -\mu_0 r \left(\frac{m_1}{r_1^3} + \frac{m_2}{r_2^3} \right) + \mu_0 m_1 D_1 \sin \varepsilon \left(\frac{1}{r_2^3} - \frac{1}{r_1^3} \right); \quad (55)$$

$$F_{Cy} = -\mu_0 r \left(\frac{m_1}{r_1^3} + \frac{m_1}{r^3} - \frac{m_1}{r^3} + \frac{m_2}{r_2^3} + \frac{m_2}{r^3} - \frac{m_2}{r^3} \right) + \mu_0 m_1 D_1 \sin \varepsilon \left(\frac{1}{r_2^3} - \frac{1}{r_1^3} \right); \quad (56)$$

$$F_{Cy} = -\mu_0 \frac{m}{r^2} + \mu_0 r m_1 \left(\frac{1}{r^3} - \frac{1}{r_1^3} \right) - \mu_0 r m_2 \left(\frac{1}{r^3} - \frac{1}{r_2^3} \right) + \mu_0 m_1 D_1 \sin \varepsilon \left(\frac{1}{r_2^3} - \frac{1}{r_1^3} \right). \quad (57)$$

By the cosine theorem

$$\begin{aligned} \frac{1}{r_2^3} - \frac{1}{r_1^3} &= \frac{1}{r^3} \left(\frac{r^2 + D_2^2 - 2rD_2 \cos(\pi/2 - \varepsilon)}{r^2} \right)^{-3/2} \\ &\quad - \frac{1}{r^3} \left(\frac{r^2 + D_1^2 - 2rD_1 \cos(\pi/2 + \varepsilon)}{r^2} \right)^{-3/2} = \\ &= \frac{1}{r^3} \left[\left(1 - \frac{2D_2 \sin \varepsilon}{r} + \frac{D_2^2}{r^2} \right)^{-3/2} - \left(1 + \frac{2D_1 \sin \varepsilon}{r} + \frac{D_1^2}{r^2} \right)^{-3/2} \right] \end{aligned} \quad (58)$$

Excluding the terms of the second order of smallness ($D \ll r$)

$$\frac{1}{r_2^3} - \frac{1}{r_1^3} \cong \frac{1}{r^3} \left[\left(1 - \frac{2D_2 \sin \varepsilon}{r}\right)^{-3/2} - \left(1 + \frac{2D_1 \sin \varepsilon}{r}\right)^{-3/2} \right]; \quad (59)$$

and applying the Newton binomial formula and discarding the terms of the second order of smallness in the expansion

$$\left(1 - \frac{2D_2 \sin \varepsilon}{r}\right)^{-3/2} \cong 1 + \frac{3D_2 \sin \varepsilon}{r}; \quad \left(1 + \frac{2D_1 \sin \varepsilon}{r}\right)^{-3/2} \cong 1 - \frac{3D_1 \sin \varepsilon}{r}; \quad (60)$$

obtain

$$\frac{1}{r_2^3} - \frac{1}{r_1^3} \cong \frac{3D \sin \varepsilon}{r^4}. \quad (61)$$

Analogically

$$\frac{1}{r^3} - \frac{1}{r_1^3} = \frac{1}{r^3} \left[1 - \left(1 + \frac{2D_1 \sin \varepsilon}{r} + \frac{D_1^2}{r^2}\right)^{-3/2} \right]; \quad (62)$$

$$\frac{1}{r^3} - \frac{1}{r_1^3} \cong \frac{1}{r^3} \left[1 - \left(1 + \frac{2D_1 \sin \varepsilon}{r}\right)^{-3/2} \right]; \quad (63)$$

$$\frac{1}{r^3} - \frac{1}{r_1^3} \cong \frac{3D_1 \sin \varepsilon}{r^4}. \quad (64)$$

As well as

$$\frac{1}{r_2^3} - \frac{1}{r^3} = \frac{1}{r^3} \left[\left(1 - \frac{2D_2 \sin \varepsilon}{r} + \frac{D_2^2}{r^2}\right)^{-3/2} - 1 \right]; \quad (65)$$

$$\frac{1}{r_2^3} - \frac{1}{r^3} \cong \frac{1}{r^3} \left[\left(1 - \frac{2D_2 \sin \varepsilon}{r}\right)^{-3/2} - 1 \right]; \quad (66)$$

$$\frac{1}{r_2^3} - \frac{1}{r^3} \cong \frac{3D_2 \sin \varepsilon}{r^4}. \quad (67)$$

From (51), (61) and (12) we obtain (9)

$$F_{Cx} = \mu_0 m_1 D_1 \cos \varepsilon \frac{3D \sin \varepsilon}{r^4}; \quad (68)$$

$$F_{Cx} = \frac{3}{2} \mu_0 \frac{mD^2}{r^4} \frac{\eta}{(1+\eta)^2} \sin 2\varepsilon.$$

From (57), (64) and (57) we obtain (11)

$$F_{Cy} = -\mu_0 \frac{m}{r^2} + \mu_0 r m_1 \frac{3D_1 \sin \varepsilon}{r^4} - \mu_0 r m_2 \frac{3D_2 \sin \varepsilon}{r^4} + \mu_0 m_1 D_1 \sin \varepsilon \frac{3D \sin \varepsilon}{r^4}; \quad (69)$$

$$F_{Cy} = -\mu_0 \frac{m}{r^2} + 3\mu_0 m_1 D_1 \frac{D}{r^4} \sin^2 \varepsilon; \quad (70)$$

$$F_{Cy} = -\mu_0 \frac{m}{r^2} + 3\mu_0 \frac{mD^2}{r^4} \frac{\eta}{(1+\eta)^2} \sin^2 \varepsilon.$$

Let us define expression (13) for the moment $M_C(\mathbf{G}_1, \mathbf{G}_2)$

$$M_C = G_1 \sin \alpha D_1 \sin \varepsilon - G_1 \cos \alpha D_1 \cos \varepsilon + G_2 \sin \beta D_2 \sin \varepsilon + G_2 \cos \beta D_2 \cos \varepsilon; \quad (71)$$

$$M_C = G_1 D_1 (\sin \alpha \sin \varepsilon - \cos \alpha \cos \varepsilon) + G_2 D_2 (\sin \beta \sin \varepsilon + \cos \beta \cos \varepsilon); \quad (72)$$

$$M_C = \mu_0 \frac{m_1}{r_1^2} D_1 (\sin \alpha \sin \varepsilon - \cos \alpha \cos \varepsilon) + \mu_0 \frac{m_2}{r_2^2} D_2 (\sin \beta \sin \varepsilon + \cos \beta \cos \varepsilon); \quad (73)$$

$$M_C = \mu_0 m_1 D_1 \left[\frac{\sin \alpha \sin \varepsilon - \cos \alpha \cos \varepsilon}{r_1^2} + \frac{\sin \beta \sin \varepsilon + \cos \beta \cos \varepsilon}{r_2^2} \right]; \quad (74)$$

$$M_C = \mu_0 m_1 D_1 \left(\frac{D_1}{r_1^3} \cos \varepsilon \sin \varepsilon - \frac{r + D_1 \sin \varepsilon}{r_1^3} \cos \varepsilon + \frac{D_1}{r_1^3} \cos \varepsilon \sin \varepsilon - \frac{r + D_1 \sin \varepsilon}{r_1^3} \cos \varepsilon \right); \quad (75)$$

$$M_C = \mu_0 m_1 D_1 r \cos \varepsilon \left(\frac{1}{r_2^3} - \frac{1}{r_1^3} \right); \quad (76)$$

$$M_C = \mu_0 m_1 D_1 \cos \varepsilon \frac{3D \sin \varepsilon}{r^3}; \quad (77)$$

$$M_C = \frac{3}{2} \mu_0 \frac{m_1 D_1 D}{r^3} \sin 2\varepsilon; \quad (78)$$

$$M_C = \frac{3}{2} \mu_0 \frac{m_1 D_1 (D_1 + D_2)}{r^3} \sin 2\varepsilon; \quad (79)$$

$$M_C = \frac{3}{2} \mu_0 \frac{(m_1 D_1^2 + m_2 D_2^2)}{r^3} \sin 2\varepsilon; \quad (80)$$

$$M_C = \frac{3}{2} \mu_0 \frac{J_D}{r^3} \sin 2\varepsilon;$$

where

$$J_D = m_1 D_1^2 + m_2 D_2^2. \quad (81)$$

References

- [1] K.E. Tsiolkovsky, Exploration of the world spaces by reactive devices: (reprinting works of 1903 and 1911 with some changes and additions), Kaluga: 1st Guest. GSNH, 1926.
- [2] I.R. Mcnab, Electromagnetic launch to space JBIS, Journal of the British Interplanetary Society, 60 (2) (2007), pp. 54-62.
- [3] M.M. Peet, The orbital mechanics of space elevator launch systems, Acta Astronautica, 179 (2021), pp. 153-171.
- [4] G. Colombo, E.M. Gaposchkin, M.D., Grossi, G.C. Weiffenbach, The «Skyhook»: A shuttle-borne tool for low-orbital-altitude research, Meccanica, 10 (1) (1975), pp. 3-20.
- [5] S. Gong, M. Macdonald, Review on solar sail technology, Astrodynamics, 3 (2), (2019), pp. 93-125.
- [6] S. Mazouffre, Electric propulsion for satellites and spacecraft: Established technologies and novel approaches, Plasma Sources Science and Technology, 25 (3) (2016), 033002.

- [7] C. Phipps, et al. Review: Laser-ablation propulsion, *Journal of Propulsion and Power*, 26 (4) (2010), pp. 609-637.
- [8] R. Shawyer, second generation EmDrive propulsion applied to SSTO launcher and interstellar probe, *Acta Astronaut.* 116 (2015) 166–174. <https://doi.org/10.1016/j.actaastro.2015.07.002>.
- [9] H. Fearn, N. van Rossum, K. Wanser, J.F. Woodward, Theory of a Mach effect thruster II, *J. Mod. Phys.* 06 (2015) 1868–1880. <https://doi.org/10.4236/jmp.2015.613192>.
- [10] M. Alcubierre, The warp drive: Hyper-fast travel within general relativity, *Classical and Quantum Gravity*, 11 (5) (1994), 001, pp. L73-L77.
- [11] V.V. Beletsky, E.M. Levin, *Dynamics of Space Tether Systems*, Univelt, San Diego, CA, 1993.
- [12] V.V. Beletsky, *Essays on the Motion of Celestial Bodies*, Birkhäuser, Basel, 2001.
- [13] A. Djebli, M., Pascal, A new method for the orbital modification of a tether connected satellite system, *Acta Mechanica*, 167 (2004), pp. 113-122. <https://doi.org/10.1007/s00707-003-0024-7>.
- [14] V.S. Aslanov, A.S. Ledkov, Swing principle in tether-assisted return mission from an elliptical orbit, *Aerospace Science and Technology*, 71 (2017), pp. 156-162.
- [15] H. Troger, A.P. Alpatov, V.V. Beletsky, V.I. Dranovskii, V.S. Khoroshilov, A.V. Pirozhenko, A.E. Zakrzhevskii, *Dynamics of Tethered Space Systems*, CRC Press, New-York, 2010.
- [16] J.V. Breakwell, J.W. Gearhart, Pumping a Tethered Configuration to Boost its Orbit Around an Oblate Planet, *Journal of the Astronautical Sciences*, 35 (1987) 19-39.
- [17] D.B. Spencer, Yu.N. Razoumny, S.A. Kupreev, Principle of motion based on the kinetic moment, *Advances in the Astronautical Sciences*, 174 (2021), 301-307.
- [18] B. Lynch, B., A. Ellery, Spacecraft propulsion using angular momentum transfer based on gravity gradient effects, *Journal of Spacecraft and Rockets*, 52 (2015), pp. 481-495. <https://doi.org/10.2514/1.A32924>.
- [19] J.D. Isaacs, A.C. Vine, H. Bradner, G.E. Bachus, Satellite elongation into a true "sky-hook", *Science*, 151 (1966) 682-683. <https://doi.org/10.1126/science.151.3711.682>.
- [20] J. Pearson, The orbital tower: A spacecraft launcher using the Earth's rotational energy, *Acta Astronautica*, 2 (1975) 785-799. [https://doi.org/10.1016/0094-5765\(75\)90021-1](https://doi.org/10.1016/0094-5765(75)90021-1).
- [21] C.D. Murray, S.F. Dermott, *Solar System Dynamics*. Cambridge University Press, UK, 1999.
- [22] L.D. Landau, E.M. Lifshitz, *Quantum Mechanics: Non-Relativistic Theory*. Pergamon Press, UK, 1977.
- [23] B.P. Abbott, 2018. Erratum: GW170104: Observation of a 50-solar-mass binary black hole coalescence at redshift 0.2. *Physical Review Letters*. 121, e129901. <https://doi.org/10.1103/PhysRevLett.121.129901>.
- [24] L. Giannessi, E. Allaria, K.C. Prince, C. Callegari, G. Sansone, K. Ueda, T. Morishita, C.N. Liu, A.N. Grum-Grzhimailo, E.V. Gryzlova, N. Douguet, K. Bartschat, 2018. Coherent control schemes

- for the photoionization of neon and helium in the Extreme Ultraviolet spectral region. *Scientific Reports*. 8, e7774. <https://doi.org/10.1038/s41598-018-25833-7>.
- [25] A.V. Belinsky, On David Bohm's 'pilot-wave' concept, *Physics-Uspekhi*, 12 (2019), pp. 1268-1278. <https://doi.org/10.3367/UFNe.2018.11.038479>.
- [26] Youtube, Slow motion video of a drop of liquid. https://www.youtube.com/watch?v=rIMQob_P9C0, 2020 (accessed 12 December 2020).
- [27] Youtube, Slow motion video of a pistol shot. <https://www.youtube.com/watch?v=hnHXk2bpArA>, 2020 (accessed 12 December 2020).
- [28] BBC, Brian Cox visits the world's biggest vacuum. <https://www.discovermagazine.com/the-sciences/watch-a-feather-and-bowling-ball-fall-at-the-same-speed>, 2020 (accessed 12 December 2020).
- [29] R. Shawyer, 2019. EmDrive thrust/load characteristics. Theory, experimental results and a moon mission. Proceedings of the International Astronautical Congress, 2019-October, eIAC-19_C4_10_14_x48783.
- [30] M. Kößling, M. Monette, M. Weikert, M. Tajmar, The SpaceDrive project - Thrust balance development and new measurements of the Mach-Effect and EMDrive Thrusters, *Acta Astronautica*, 161 (2019) 139-152, <https://doi.org/10.1016/j.actaastro.2019.05.020>.
- [31] H. Fearn, N. van Rossum, K. Wanser, J.F. Woodward, Theory of a Mach effect thruster II, *J. Mod. Phys.* 06 (2015) 1868–1880, <https://doi.org/10.4236/jmp.2015.613192>.
- [32] S. Capozziello, M. de Laurentis, Extended Theories of Gravity, *Physics Reports*, 509 (4-5) (2011), pp. 167-321.
- [33] K. Becker, M. Becker, J.H. Schwarz, *String Theory and M-Theory: A Modern Introduction*, pp. 1-739, 2006.
- [34] A. Ashtekar, P. Singh, Loop quantum cosmology: A status report, *Classical and Quantum Gravity*, 28 (21) (2011), 213001,
- [35] S.P. Kumar, M.B. Plenio, 2020. On quantum gravity tests with composite particles. *Nature Communications*. 11, e3900. <https://doi.org/10.1038/s41467-020-17518-5>.
- [36] B.D. Wood, G.A. Stimpson, J.E. March, Y.N.D. Lekhai, C.J. Stephen, B.L. Green, and, ...: 2021, Matter and spin superposition in vacuum experiment (MASSIVE), arXiv:2105.02105.
- [37] G.M. Tino, 2021. Testing gravity with cold atom interferometry: results and prospects. *Quantum Science and Technology*, 6 (2), 024014, <https://doi.org/10.1088/2058-9565/abd83e>.
- [38] T. Westphal, H. Hepach, J. Pfaff, M. Aspelmeyer, Measurement of gravitational coupling between millimetre-sized masses. *Nature*. 2021 Mar;591(7849):225-228, <https://doi.org/10.1038/s41586-021-03250-7>. Epub 2021 Mar 10. PMID: 33692556.

- [39] X.C. Duan, 2016. Test of the Universality of Free Fall with Atoms in Different Spin Orientations. *Physical Review Letters*. 117,2 (2016): 023001, <https://doi.org/10.1103/PhysRevLett.117.023001>.
- [40] R. Caravita, 2019. The AEGIS experiment at CERN: Probing antimatter gravity. *Nuovo Cimento c-colloquia and communications in physics* 42(2-3), 123. <https://doi.org/10.1393/ncc/i2019-19123-9>.
- [41] P. Asenbaum, C. Overstreet, M. Kim, J. Curti, M.A. Kasevich, 2020. Atom-Interferometric Test of the Equivalence Principle at the 10-12 Level. *Physical Review Letters*, 125 (19), 191101, <https://doi.org/10.1103/PhysRevLett.125.191101>.
- [42] C.G. Provatidis, Free fall of a symmetrical gyroscope in vacuum, *European Journal of Physics*, 42 (6) (2021), № 065011.
- [43] B.P. Abbott, 2016. Tests of General Relativity with GW150914. *Physical Review Letters*. 116, 22 (2016): 221101. <https://doi.org/10.1103/PhysRevLett.116.221101>.
- [44] J. Cervantes-Cota, S. Galindo-Uribarri, G. Smoot, 2016. A Brief History of Gravitational Waves. *Universe* 2, 22.. <https://doi.org/10.3390/universe2030022>.
- [45] A.B. Aleksandrov, A.B. Dashkina, N.S. Konovalova, N.M. Okat'eva, N.G. Polukhina, N.I. Starkov and, ...: 2021. Search for weakly interacting massive dark matter particles: state of the art and prospects, *Physics-Uspekhi*, 64(9). pp. 861-889. <https://doi.org/10.3367/UFNe.2020.11.038872>.